Cell, Vol. 99, 367–376, November 12, 1999, Copyright ©1999 by Cell Press

Control of Organ Asymmetry in Flowers of *Antirrhinum*

Da Luo,† Rosemary Carpenter, Lucy Copsey, Coral Vincent, Jennifer Clark, and Enrico Coen*
Genetics Department
John Innes Centre
Colney Lane
Norwich NR4 7UH
United Kingdom

Summary

Organ asymmetry is thought to have evolved many times independently in plants. In *Antirrhinum*, asymmetry of the flower and its component organs requires *cyc* and *dich* gene activity. We show that, like *cyc*, the *dich* gene encodes a product belonging to the TCP family of DNA-binding proteins that is first expressed in the dorsal domain of early floral meristems. However, whereas *cyc* continues to be expressed throughout dorsal regions, expression of *dich* eventually becomes restricted to the most dorsal half of each dorsal petal. This correlates with the effects of *dich* mutations and ectopic *cyc* expression on petal shape, providing an indication that plant organ asymmetry can reflect subdomains of gene activity. Taken together, the results indicate that plant organ asymmetry can arise through a series of steps during which early asymmetry in the developing meristem is progressively built upon.

Introduction

There are many cases in which the left and right halves of a plant organ have distinct shapes. Examples of such organ asymmetry include the leaves of *Begonia*, *Tilia* (lime tree), and *Ulmus* (elm) and the petals of *Antirrhinum* (snapdragon) or *Pisum* (pea) flowers. Asymmetric organs can potentially occur in two mirror-image forms, left-handed and right-handed. In many cases, these two forms occur in equal numbers on the plant, either being located opposite each other or alternating along the stem (pendulum symmetry; Charlton, 1998). This suggests that the asymmetry of each organ traces back to a meristem with a single plane of symmetry (bilateral symmetry), such that organs with opposite handedness arise from opposite halves of the meristem, much as the asymmetry of an animal limb can be traced back to the earlier bilateral symmetry of the embryo (Wolpert et al., 1998). However, unlike the situation in animals, where limb asymmetry evolved at a very early stage of evolution, organ asymmetry in flowering plants is thought to have evolved more recently and many times independently. This raises the question of how organ asymmetry is established in plants and how it might have been coupled to meristem development during evolution. To address some of these problems, we have analyzed the molecular genetic basis of petal asymmetry in flowers of *Antirrhinum*.

Wild-type *Antirrhinum* flowers exhibit marked differences in petal shape along their dorsoventral axis and have a single plane of symmetry (Figure 1). Each flower has five petals: a pair of dorsal (upper) petals, a pair of lateral (side) petals, and one ventral (lowest) petal. The dorsal and lateral petals are individually asymmetric, while the ventral petal has bilateral symmetry, being bisected by the dorsoventral axis. Dorsoventral asymmetry is also evident for the stamens: the dorsal stamen is arrested to form a staminode, and the pair of lateral stamens are shorter than the ventral stamens. Mutant lines of *Antirrhinum* have been described in which all petals and stamens resemble their ventral counterparts in wild type (peloric phenotype), rendering the flower radially symmetrical and eliminating individual organ asymmetry. These peloric lines can result from mutations in two genes: *cycloidea* (*cyc*) and *dichotoma* (*dich*) (Carpenter and Coen, 1990; Luo et al., 1996; Almeida et al., 1997). Mutations in *cyc* alone give an intermediate phenotype (semipeloric), in which the petals in lateral positions have a ventral identity, while those in dorsal positions have a combination of dorsal and lateral characteristics. Mutations in *dich* alone have a more subtle effect, only altering the shape of the dorsal petals (Kuckuck and Schick, 1930; Stubbe, 1966). The *cyc* gene has been characterized and shown to encode a product belonging to the TCP family of DNA-binding proteins (Luo et al., 1996; Doebley et al., 1997; Kosugi and Ohashi, 1997; Cubas et al., 1999). Expression of *cyc* is first detected in the dorsal domain of early floral meristems, before organ primordia are visible. Expression then continues through to later stages of development in dorsal petals and the dorsal stamen (staminode).

Here we describe the function and isolation of *dich*. We show that the predicted DICH protein is closely related to CYC, accounting for the partial redundancy of *dich* and *cyc* in the control of flower asymmetry. The *dich* and *cyc* genes also exhibit a similar early expression pattern, being first detected in the dorsal domain of the floral meristem. However, at later stages, *dich* expression becomes restricted to the most dorsal half of each dorsal petal, unlike *cyc*, which continues to be expressed throughout most of the dorsal domain. Taken together with the phenotype of *dich* mutants, this suggests that the normal role of *dich* is to confer distinctions between the halves of each dorsal petal, making each petal more asymmetric. In support of this model, we show that ectopic expression of *cyc* alone results in the lower three petals developing as mirror-image duplications of the lateral half of the dorsal petals. We propose that petal asymmetry arises through a series of steps in which gene expression patterns are progressively

*To whom correspondence should be addressed (e-mail: coenen@bbsrc.ac.uk).
† Present address: National Laboratory of Plant Molecular Genetics, Shanghai Institute of Plant Physiology, The Chinese Academy of Sciences, 300 Fenglin Road, Shanghai 200032, China.

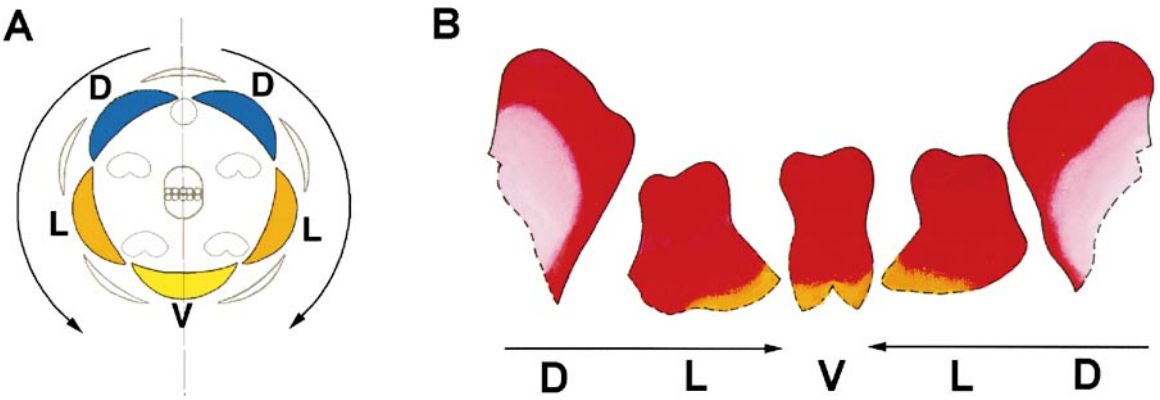

Figure 1. Floral Diagram and Petal Lobes of Wild-Type *Antirrhinum*

(A) Schematic transverse section through an *Antirrhinum* flower showing a single plane of symmetry (dotted line) running along the dorsoventral axis. Each flower has five petals: a pair of dorsals (D), a pair of laterals (L), and one ventral (V). The petals are highlighted in different colors, while the other flower organs (sepals, stamens, and central carpels) are shown in gray outline. The arrows running from dorsal to ventral around the diagram indicate its relationship to the flattened representation shown in (B), where the corresponding arrows are straight.

(B) Diagram of the petal lobes, cut off the flower and flattened out to reveal the front (adaxial) surface (dotted lines indicate the sites of cutting). The arrows along the bottom correspond to those around the floral diagram of (A). The dorsal and lateral lobes are individually asymmetric, while the ventral petal has bilateral symmetry, being bisected by the dorsoventral axis.

elaborated and maintained, from early meristem initiation through late stages of development.

It is possible that this developmental progression also reflects a sequence of evolutionary events. Asymmetric patterns of gene expression in meristems could have arisen at an early stage of flowering plant evolution, presumably with a distinctive role in meristem development. This ancestral asymmetry could then have been recruited and built upon several times independently during evolution to generate organ asymmetry later in development.

Results

Phenotype and Isolation of *dich*

In mutants homozygous for the classical *dich*^{G} allele, the dorsal petal lobes had a more symmetrical appearance than in wild type and were typically separated from each other by a deep divide (Figures 2A–2D; Kuckuck and Schick, 1930; Stubbe, 1966). The junction between the dorsal lobes and the tube in *dich*^{G} mutants was also more rounded. The veins in the dorsal petals were more symmetrically distributed than in wild type, particularly in the distal regions (Figures 2E and 2F). In a flattened dorsal petal of wild type, the veins in the more dorsal half were densely packed and bent toward the middle of the flower, while in *dich*^{G} the corresponding veins were less curved and had a more open pattern, similar to the other half of the dorsal petal. The phenotype was more variable in the *dich-717* and *dich-719* mutants, both of which were initially identified as peloric variants within a *cyc* mutant background during a transposon-mutagenesis experiment (Carpenter and Coen, 1990; Luo et al., 1996). In mature flowers of *dich*^{G} mutants, the arrested dorsal stamen (staminode) was generally longer than in wild type. Unlike *cyc* mutants, there was no increase in the number of petals or stamens in *dich* mutants.

The development of *dich*^{G} was compared to that of wild type by scanning electron microscopy (SEM). Flower meristems arise sequentially on the periphery of the inflorescence apex, such that the youngest stage of development (node 0) is nearest the apex and progressively older stages occur below this (Carpenter et al., 1995). Altogether, there are about 60 nodes between the earliest stage and the mature flower. There were no detectable differences between *dich*^{G} and wild-type meristems up to stage 7 (about node 30), even though the petal lobe primordia were clearly visible (data not shown). However, by stage 8 (about node 35), *dich* mutants could be distinguished from wild type by the more symmetrical appearance of the two dorsal lobes and the divide between them (Figures 2G and 2I). This distinction was maintained during later stages (Figures 2H and 2J). Thus, the phenotypic effects of *dich* only become apparent when the flower was about halfway through its development.

Since genetic analysis had revealed that both *dich* and *cyc* were needed to establish full dorsoventral asymmetry (Luo et al., 1996; Almeida et al., 1997), we investigated the possibility that the *dich* gene sequence could be related to that of *cyc*. A cDNA library was probed at low stringency with the *cyc* open reading frame (ORF), yielding a clone containing an ORF encoding a predicted protein with 77% similarity to that of *cyc*. Using this *cyc*-like cDNA to probe DNA blots, we showed that all three *dich* mutants (*dich-717*, *dich-719*, and *dich*^{G}) had banding patterns that were distinct from their wild-type progenitors, suggesting that each of them contained an alteration at the *cyc*-like locus (Figure 3). Based on restriction enzyme mapping, the three *dich* alleles were shown to have been generated by insertions, most probably transposons (Figure 4A). The rate of transposon integration in *Antirrhinum* is normally well below 10^{-3} per locus, so the probability that these insertions could have arisen by chance in both *dich-717* and *dich-719* (which could be directly compared to their immediate progenitors) was less than 10^{-6}. To test

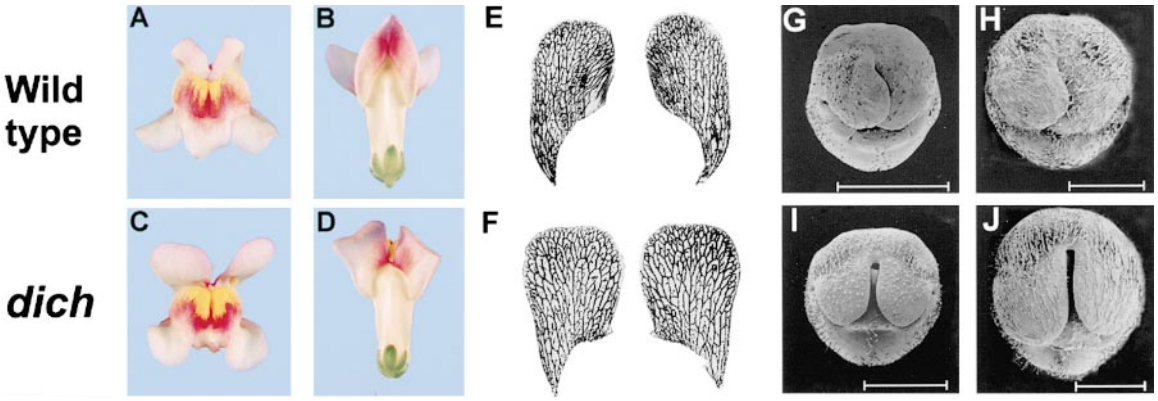

Figure 2. Phenotype and Development of *dich*^{G}

(A–D) Comparison between mature flowers of wild type and *dich*^{G} viewed from the front (A and C) or from above (B and D). Note the deeper divide between the dorsal petal lobes of *dich*^{G}.

(E and F) Venation pattern and shape of flattened dorsal lobes from flowers of wild type (E, Sippe 50) and *dich*^{G} (F) showing the back (abaxial) surface. The individual lobes of *dich*^{G} have a more symmetrical shape and venation pattern, particularly in the more distal regions (upper parts of the petal in the figure).

(G–J) SEMs of wild-type (top) and *dich*^{G} (bottom) at stages 8 (G and I) and 9 (H and J) of development (about nodes 35 and 40, respectively). The dorsal petals of wild type overlap at these stages, while those of *dich*^{G} are separated by a clear divide and have a more symmetrical shape. The sepals have been removed. Bar, 1 mm.

whether these insertions were linked to *dich*, two families segregating for *dich* alleles in a *cyc-608* genetic background were probed with the *cyc*-like gene (in a *cyc* background, *dich* gives a peloric phenotype and can be semidominant [Carpenter and Coen, 1990; Luo et al., 1996; Almeida et al., 1997]). In all cases, plants with a peloric phenotype were either homozygous or heterozygous for insertions in the *cyc*-like gene (data not shown). Taken together, these results indicated that the *cyc*-like gene corresponded to *dich*.

A genomic library was screened with the *dich* cDNA to obtain a clone of the *dich* locus. Two overlapping clones were obtained and sequenced. This revealed an uninterrupted ORF encoding a putative DICH protein of 314 amino acids, which was 66% identical to CYC (Figures 4A and 4B). The two most conserved regions were the TCP domain, shared by a family of DNA-binding proteins, and the R domain, named for its richness in arginine residues (Figure 4B; Cubas et al., 1999). A putative bipartite nuclear localization signal inside the TCP domain was also conserved (Dingwall and Laskey, 1991; Luo et al., 1996; Cubas et al., 1999). 5′ and 3′ RACE showed that *dich* had two exons. There was no extensive homology between the *dich* and *cyc* loci outside the ORF, although some patches of similarity were detected upstream of the transcription start sites of both genes. No other putative coding regions were identified when the sequence of 15 kb around the *dich* locus was analyzed.

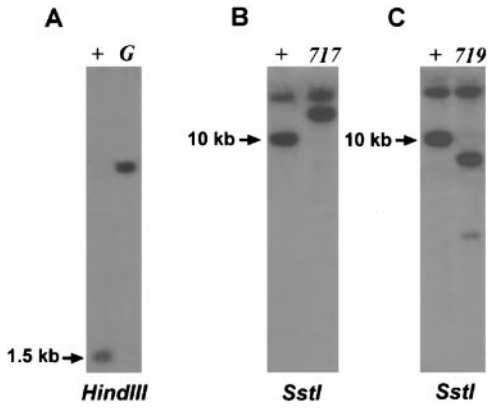

Figure 3. Various *dich* Mutants Probed with the *cyc*-like cDNA

Genomic DNAs from *dich*^{G}, *dich-717*, *dich-719*, and their wild-type progenitors (+) were digested with either HindIII or SstI and blotted. The blots were probed with a 1.3 kb fragment from pJAM2078, which contains the *cyc*-like ORF.

(A) The *dich*^{G} mutant (G) gave a 7.5 kb band compared to 1.5 kb in its progenitor.

(B and C) Both *dich-717* and *dich-719* gave novel bands compared to the 10 kb band in their wild-type progenitor.

PCR analysis showed that the *dich*^{G} allele had a transposon insertion with a perfect 8 bp inverted repeat at its ends, flanked by a 5 bp target duplication at the insertion site within the ORF (Figure 4A). The terminal regions of the transposon contained long direct repeats of about 130 bp. The *dich-717* and *dich-719* alleles carried insertions several kilobases downstream of the second exon of *dich* (Figure 4A). A peloric mutant, JI25, which also carries a *dich* mutation (Luo et al., 1996), contained an insertion very near the 3′ end of the *dich* transcribed region.

Expression Pattern of *dich* in Wild-Type and Mutant Backgrounds

The expression pattern of *dich* was characterized by RNA in situ hybridization and compared to that of *cyc*. Digoxigenin-labeled antisense *dich* and *cyc* probes were hybridized to alternate serial sections of wild-type or mutant inflorescence apices, each containing several stages of floral development (Carpenter et al., 1995).

In wild type, expression of *dich* could be observed as early as stage 1 (node 3), when the signal was detected

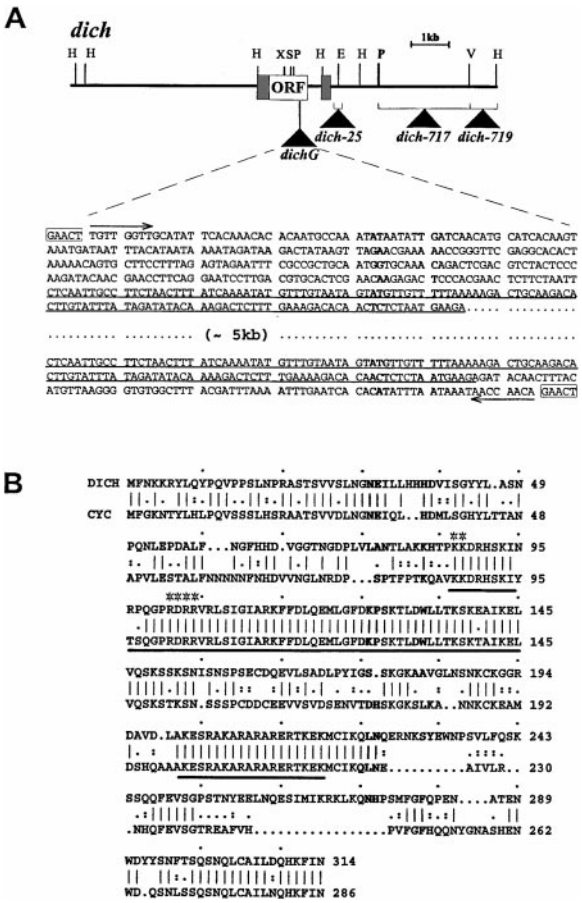

Figure 4. Structure and Sequence of *dich*

(A) Map of the *dich* locus. The exons and predicted ORF are indicated as rectangles. Black triangles represent the transposon insertions for different *dich* alleles. Only the insertion site for *dich*^{G} was precisely determined by sequencing. The others were mapped to the fragments indicated. The transposon insertion in *dich*^{G} is shown below. Target duplications produced by the transposon are boxed in, inverted repeats of the transposon are indicated with arrows, and long repeats of the transposon are underlined. E, EcoRI; V, EcoRV; H, HindIII; P, PstI; S, SstI; X, XhoI. (B) Deduced amino acid sequence of DICH and its alignment with CYC. The putative bipartite motif similar to a consensus nuclear localization signal (Dingwall and Laskey, 1991) is indicated with stars. The TCP domain and the R domain (Cubas et al., 1999) are underlined. The alignment was carried out by using the Bestfit program (GCG Software).

in a few cells at the junction between the inflorescence meristem and the floral meristem (data not shown). After this, during stages 2–5, expression of *dich* was restricted to the dorsal region of the floral meristem (Figures 5D and 5E). After stage 6, when petal and stamen primordia were formed, expression was observed in the dorsal petals and staminode (Figure 5F).

Although this expression pattern was very similar to that of *cyc* (Luo et al., 1996), probing adjacent sections with *cyc* and *dich* revealed several differences. First, *dich* expression was detectable one or two nodes earlier than *cyc*, indicating that *dich* was activated slightly before *cyc*. Second, by stage 4, when petal and stamen primordia were initiating, *cyc* expression was concentrated in regions where the primordia of dorsal petals and staminode were forming, while *dich* expression seemed to be spread more evenly in the dorsal region (Figures 5B and 5E). Third, at later stages, *dich* expression was restricted to the dorsal half of each dorsal petal, whereas *cyc* expression extended throughout most of each dorsal petal (Figures 5C and 5F).

After stage 7, the signal for both *dich* and *cyc* became weaker and more difficult to detect by in situ hybridization. To determine the pattern of *dich* expression in more mature flowers, petal lobes from flower buds of different sizes (9, 12, or 18 mm long) were dissected and the transcripts of *dich* and *cyc* assayed by RT–PCR. As expected, both *dich* and *cyc* were expressed only in the dorsal petals of flower buds (Figure 6). Consistent with the in situ hybridization data, the expression domain of *dich* was smaller than that of *cyc*: expression of *dich* was mainly confined within the dorsal half (Dd) of the dorsal petals, while strong *cyc* expression was detectable in both halves (Dd and Dl) of the dorsal petals (Figure 6).

The expression patterns of *cyc* in the *dich*^{G} mutant and of *dich* in the *cyc-608* mutant were indistinguishable from those in wild type. There was no detectable *dich* expression either in *dich*^{G} mutants or in the peloric line JI25 carrying *dich-25* (data not shown).

Phenotype and Expression Pattern of the *backpetals* Mutant

The phenotype and expression pattern of *dich* indicated that it had a role in establishing distinctions between the two halves of each dorsal of wild type. To test this further, we analyzed a novel mutant, *backpetals*, which also had a phenotype suggesting that the halves of each dorsal petal might be under separate genetic control. In contrast to the previously described semipeloric or peloric mutants, which are ventralized, in the *backpetals* mutant, the lateral and ventral petals were dorsalized: the overall size and cell types of the petal tube and lobe regions resembled those of dorsal petals (Figures 7C and 7D). Closer examination of the shape, cell types, and venation patterns of these petals showed that they resembled mirror-image duplications of only the lateral half (Dl) of the normal dorsal petal (Figures 7J–7M; see legend for details). The *backpetals* phenotype was often variable; in some plants, flowers from the same spike could be *backpetals*, wild type, or intermediate. In the intermediate flowers, only parts of the lateral or ventral petals showed transformation toward dorsal petals. The mutant phenotype was attenuated when plants were grown at higher temperature (25°C). The *backpetals* mutation is semidominant: when crossed to a wild-type line (JI98), it gave F_1 plants with a weak mutant phenotype. Often only part of a petal was dorsalized in heterozygotes, the dorsalization commonly involving petal regions nearest to the dorsal petals, as if dorsal identity was "spreading" out from the dorsal domain into the adjacent lateral region (Figure 7E). The *backpetals* mutant was genetically unstable, occasionally giving revertant progeny. There was no obvious difference in the number of stamens in the *backpetals* mutant compared to wild type.

SEM analysis showed that flower development in the *backpetals* mutant was indistinguishable from that of

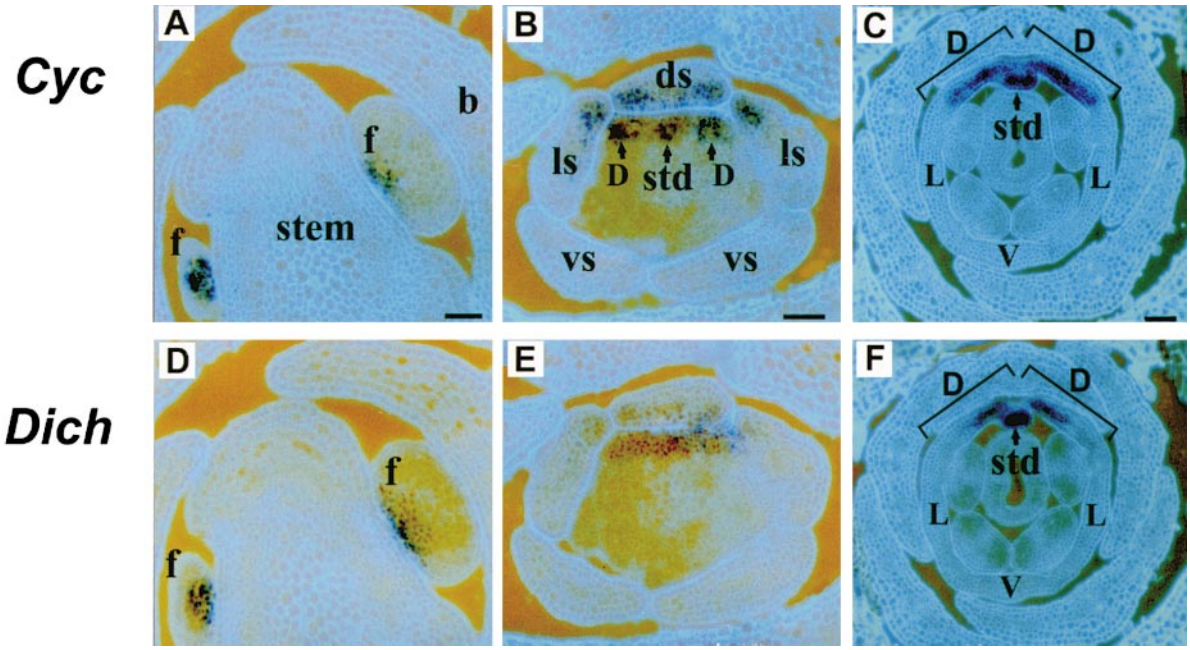

Figure 5. RNA In Situ Hybridization of Wild-Type Transverse Sections Probed Alternately with *cyc* or *dich*

(A and D) Floral meristems at stage 2, showing expression of both *cyc* and *dich* in the dorsal region. Bract (b) and floral meristems (f) are labeled.

(B and E) Stage 5 meristem, showing expression of *cyc* and *dich* in the dorsal regions. The *cyc* signal is concentrated in primordia of dorsal sepal (ds), part of the lateral sepals (ls), dorsal petals (D), and staminode (std). The ventral sepals are labeled (vs). The *dich* signal is in a comparable region but more spread out.

(C and F) Late stage 6 meristem, showing expression of both *cyc* and *dich* in dorsal petals (D) and staminode (std). Note that the expression domain of *dich* in petals is more restricted than for *cyc*. Lateral (L) and ventral (V) petals are also indicated. Bars, 100 μm.

wild type up to stage 6, when all the floral organ primordia had been initiated. However, by stage 7 (about node 30), the *backpetals* mutant could be distinguished from wild type by the larger size and rounder shape of the petals in lateral positions (Figures 7F and 7H). By stage 8, the petal lobes in lateral and ventral positions of *backpetals* resembled dorsal lobes, although they had a more symmetrical shape (Figures 7G and 7I). Also at this stage, a furrow formed at the tube–lobe junction of wild-type lateral and ventral petals, whereas no such furrow formed in *backpetals* flowers, consistent with their dorsalized phenotype.

Because the *backpetals* mutant displayed a change in dorsoventral asymmetry, we expected that the expression pattern of *dich* or *cyc* might be altered. RNA in situ hybridization failed to detect abnormal expression pattern of either *dich* or *cyc* in the early stages of floral development (stage 4, Figure 8A). However, by stage 6, patches of ectopic *cyc* expression could be seen in lateral petals (arrowed in Figure 8B). RT–PCR analysis on dissected petals from more mature flower buds showed that the *cyc* expression domain had expanded into the lateral and ventral petals, while the expression pattern of *dich* was unchanged (Figure 8C). Therefore, *cyc* was ectopically expressed in the lower petals at later stages of flower development in *backpetals* mutants.

backpetals Is Caused by a Transposon Insertion in the *cyc* Locus

The ectopic expression of *cyc* in the *backpetals* mutant, together with its semidominance, suggests that a *cis* element in the *cyc* locus may have been altered. Comparison of the *cyc* locus in *backpetals* with that of its progenitor (JI98) showed that there was a 5 kb transposon inserted in the promoter region of *cyc*, 4.2 kb upstream from the transcription start site (Figure 8D). The sequence around the insertion site was AT-rich and contained no extensive open reading frames. In revertants of *backpetals*, the transposon had excised, showing that the insertion was responsible for the *backpetals* phenotype. Thus, the *backpetals* mutant proved to be a semidominant mutation at the *cyc* locus, subsequently named *cyc-705*. One imprecise excision event was also detected, which still gave the *backpetals* phenotype. In this event, only 180 bp of one end of the transposon remained and about 70 bp of the *cyc* locus adjacent to the transposon had been deleted (data not shown).

Discussion

We have shown that asymmetry of the dorsal petals of *Antirrhinum* flowers involves activity of the *dich* gene: in *dich* mutants, these petals are more symmetrical than in wild type. The *dich* gene also plays a role in dorsal stamen development, as the staminodes are larger in *dich* mutants. The DICH protein is closely related to CYC (66% identity), lying within the TCP family of DNA-binding proteins. DICH acts together with CYC to establish dorsoventral asymmetry across the flower as a whole (*cyc:dich* double mutants are fully ventralized), indicating that the effect of *dich* on petal asymmetry is

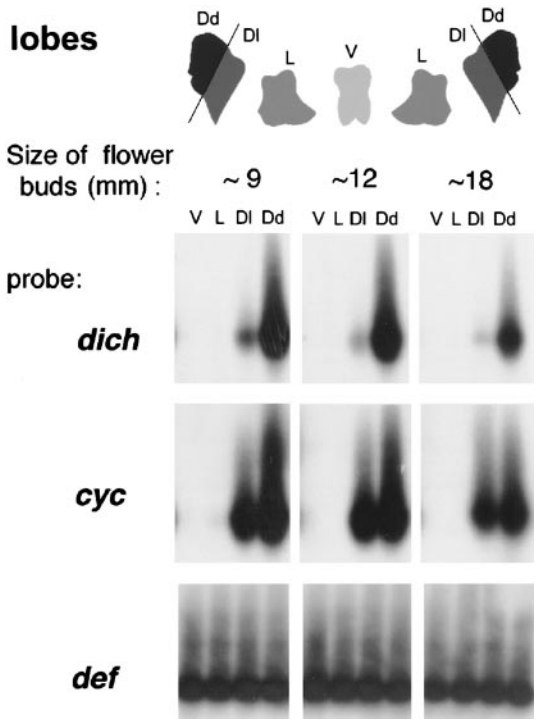

Figure 6. Expression Pattern of *dich* and *cyc* Analyzed by RT–PCR

Lobes were individually dissected from flower buds at late development stages. The dorsal petals were further dissected into two parts: dorsal (Dd) and lateral (Dl) halves, as indicated in the top diagram. RNA was extracted from lobes and RT–PCR conducted to amplify transcripts of *dich* and *cyc*. The transcript of *deficiens* (*def*) (Sommer et al., 1990), an organ identity gene that is expressed in all petals, was used as a control. The transcripts were detected by Southern hybridization using probes prepared from ORFs of these genes. Note that the transcripts of *dich* are most abundant in the dorsal half (Dd) of the dorsal petal, whereas *cyc* is abundant in both halves of the dorsal petal.

related to the overall dorsoventral asymmetry of the flower. However, unlike *cyc*, which affects the development of all petals, the effects of *dich* are restricted to petals in dorsal positions. Furthermore, whereas *cyc* mutants often show an increase from five to six organs per whorl, *dich* has little effect on flower organ number. These differences suggest that following an ancestral gene duplication, *cyc* and *dich* have diverged with respect to particular functions, even though they retain a common role in dorsoventral asymmetry.

The *dich* gene, like *cyc*, is first expressed in the dorsal domain of the flower meristem at a very early stage in development, before floral organ primordia have emerged. At later stages, when organ primordia are visible (stage 5), *dich* expression is observed in primordia of the dorsal petals and staminode. After this, *dich* expression in petals becomes restricted to the most dorsal half of each dorsal organ, a pattern that is maintained to the final stages of development. This is in contrast to *cyc*, which has a more extended domain of expression, spanning most of the dorsal petals. Thus, the *dich* expression pattern provides an example of asymmetry in gene activity between the two halves of a plant organ. One model is that *cyc* expression promotes dorsal identity throughout the dorsal petals, while *dich* activity confers a further distinction between the two halves of each dorsal petal (Figure 9A). In *dich* mutants, *cyc* activity alone remains so the dorsal petals are more symmetrical (Figure 9B). However, the dorsal petals are not completely symmetrical in *dich* mutants, indicating that other factors, possibly dependent on *cyc*, are also involved in establishing their asymmetry.

Further support for this model comes from analysis of a semidominant mutant, *backpetals*. In this mutant, the petals in dorsal positions are normal, but those in lateral and ventral positions are dorsalized. The dorsalized petals appear to consist of mirror-image duplications of the lateral half of the normal dorsal petal (Figure 9C). The *backpetals* mutant is caused by a transposon insertion in the *cyc* locus, about 4.2 kb upstream of the *cyc* transcribed region. The insertion leads to ectopic expression of *cyc* in lateral and ventral positions at later stages of development. Because expression of *cyc* but not *dich* is affected, the lower three petals assume the same identity as the lateral half of the dorsal petal (i.e., the region that normally expresses *cyc* alone), whereas the upper two petals retain their internal asymmetry conferred by *dich*. These results show that *cyc* activity is sufficient to promote dorsal identity within the context of the flower. Moreover, they confirm that *dich* activity in the upper half of the dorsal petal is separable from that of *cyc*.

How does the transposon insertion in the *backpetals* mutant lead to ectopic *cyc* expression? One possibility is that the transposon carries an enhancer that drives expression of the nearby *cyc* gene. However, a derivative of *backpetals* in which most of the transposon (together with 67 bp of adjacent sequence from *cyc* locus) has been deleted still confers the dorsalized phenotype, indicating that most of the transposon sequence is irrelevant. A more likely explanation is that the transposon insertion disrupts a *cis*-acting region that normally represses *cyc* transcription in the lateral and ventral regions at late stages of development. In the *backpetals* mutant, *cyc* is therefore derepressed, leading to the lower three petals acquiring dorsal characteristics. This type of mechanism has been proposed to account for *cis*-acting mutations in *Drosophila* that result in ectopic expression of homeotic genes. For example, *Mcp* and *Fab* are gain-of-function mutations in the Bithorax complex that result in ectopic expression of *Abdominal-B* (*Abd-B*) (Celniker et al., 1990; Gyurkovics et al., 1990; Sanchez-Herrero, 1991). They are caused by deletions downstream of the *Abd-B* gene, which remove silencing elements recognized by the Polycomb group of proteins (Busturia and Bienz, 1993; Zink and Paro, 1995; Mihaly et al., 1997). As with *backpetals*, the mutations can be many kilobases away from the transcribed region of the gene, and ectopic expression seems to spread most readily to regions adjacent to the normal expression domain. Moreover, in both *backpetals* and Polycomb group mutants, early gene expression is normal; it is only the later maintenance of the expression pattern that appears to be affected (Simon et al., 1992). Based on these similarities, it seems likely that the *backpetals* mutation disrupts *cis*-acting silencers of *cyc* that normally act to keep the gene off in lateral and ventral petals at late

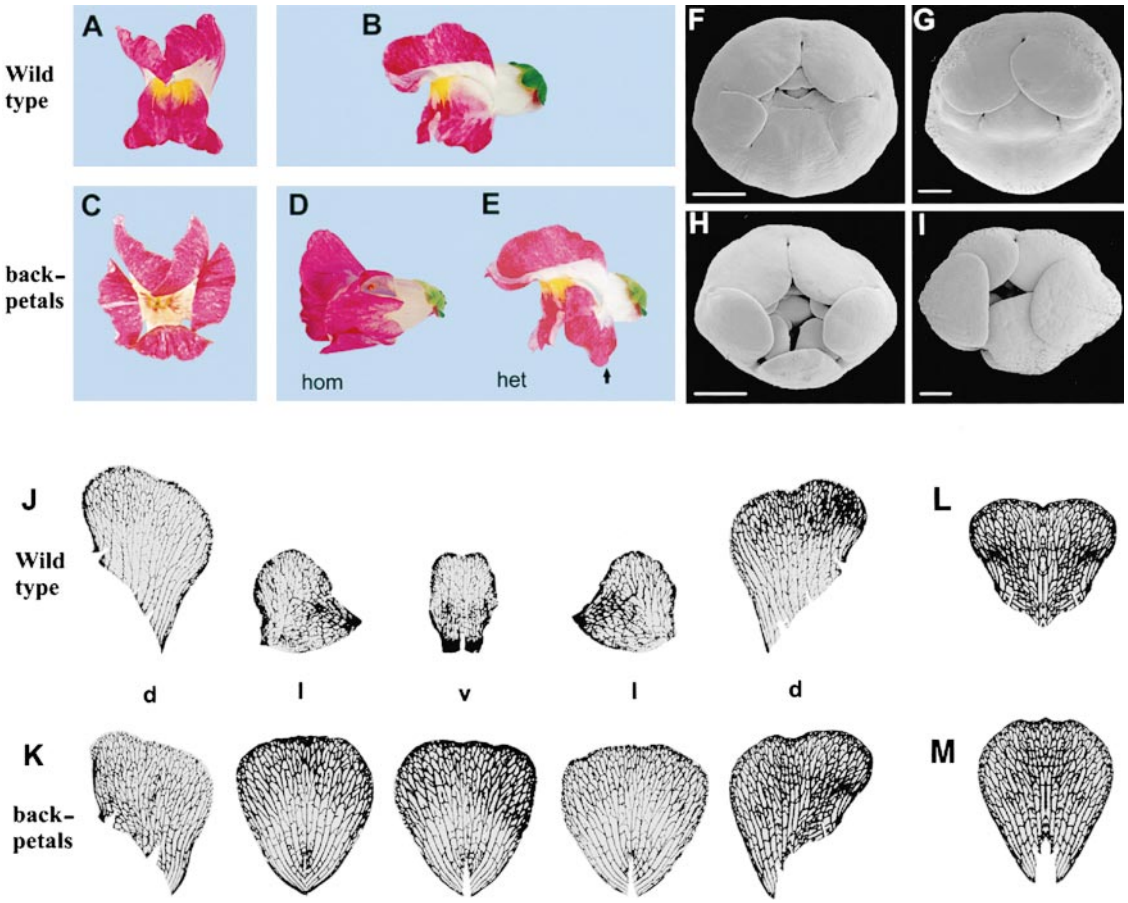

Figure 7. Phenotype of *backpetals* Compared to Wild Type

(A–E) Flowers of the wild type and *backpetals* are shown in face view (A and C) or side view (B, D, and E). The face view shows how the petals in lateral and ventral positions become dorsalized in *backpetals*. The flowers of *backpetals* heterozygotes often show only partial dorsalization, most commonly involving the region nearest to the dorsal petals, as illustrated by the heterozygote shown in (E) (see arrow).

(F–I) SEM of wild-type (top) and *backpetals* (bottom) flower buds at stages 7 (F and H) and 8 (G and I) of development.

(J–M) The shape and venation of lobes of wild-type (JI98), *backpetals*, and artificial mirror-image duplications. In *backpetals*, the dorsal petals are similar to wild type, while the other petals become symmetrical and dorsalized (J and K). Each half of these symmetrical petals has a length, shape, and venation pattern similar to that of the lateral half of the dorsal petal. This can be seen by comparing these petal lobes to ones in which the two halves of a dorsal petal have been artificially duplicated (L and M). A petal lobe derived from a duplicated lateral half (M) resembles the symmetrical petal of the *backpetals* mutant much more closely than the duplicated dorsal half (L). Similar considerations apply to the petal tube regions.

stages of development. These silencers might be recognized by proteins such as CURLY LEAF that belong to the Polycomb group and repress later expression of floral homeotic genes in *Arabidopsis* (Goodrich et al., 1997).

The effects of *cyc* and *dich* on flower shape can be viewed as the outcome of a series of steps in which asymmetry is progressively elaborated during development. A basic feature of apical meristems is the distinction between the central apical meristem and its periphery where primordia and secondary meristems initiate. This asymmetry along the radial axis of the apex is thought to originate during early embryogenesis. The dorsoventral asymmetry of the flower can be thought of as an extension of this basic radial asymmetry because the dorsal domain of the flower meristem lies nearer to the main apex than the rest of the flower. Thus, the radial asymmetry of the apex may provide a primary frame of reference for establishing the asymmetric expression of *cyc/dich* in early floral meristems (Coen, 1996). Following the establishment of *cyc/dich* activity in the dorsal domain, asymmetry may be further elaborated along the dorsoventral axis to give dorsal, lateral, and ventral domains. After this, when floral organ primordia start to form, a further stage of elaboration may be the division of these primordia into subdomains, such as the subdivision of each dorsal petal into a dorsal half expressing *dich* and *cyc*, and a lateral half expressing *cyc* alone. Some of these expression patterns may then be maintained during later periods of development by the action of genes, such as those belonging to the Polycomb group.

It is possible that this developmental progression also reflects a sequence of evolutionary events. Asymmetric patterns of gene expression in meristems could have arisen early on in the evolution of flowering plants. This

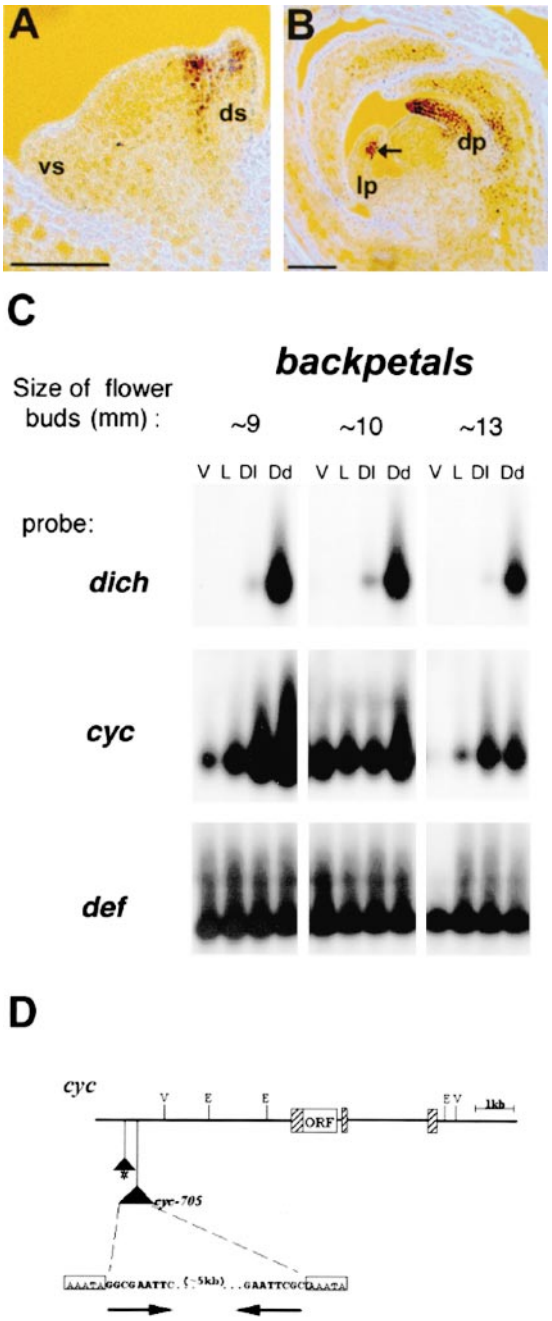

Figure 8. Expression of *dich* and *cyc* in *backpetals* and Structure of Mutant Locus

(A and B) At stage 4, *cyc* expression detected by RNA in situ hybridization is normal (A), but by stage 6, patches of *cyc* expression can be see in the lateral petals (arrowed in [B]). vs, ventral sepal; ds, dorsal sepal; lp, lateral petal; dp, dorsal petal. Bars, 100 μm.

(C) RT–PCR shows that in *backpetals*, *cyc* is ectopically expressed in the lateral and ventral petals, while *dich* expression is unaltered. Methods and symbols are as described in Figure 6.

(D) Structure of the *cyc* locus in *backpetals*. Exons and predicted ORF of *cyc* are indicated as rectangles. Black triangles represent transposon insertions. A transposon insertion present in both the wild-type progenitor (JI98) and *backpetals* is indicated by the solid triangle with a star. E, EcoRI; V, EcoRV. The sequence around the transposon insertion site in *backpetals* (*cyc-705*) is shown with the target duplication boxed in; the inverted repeats of the transposon are indicated with arrows.

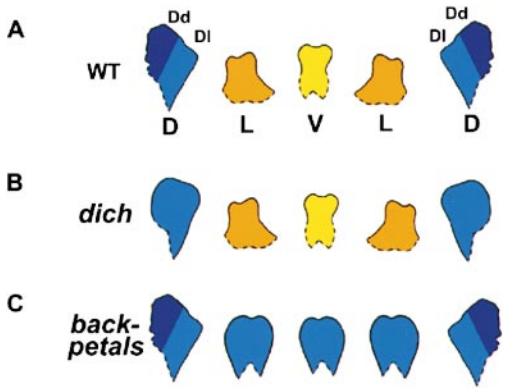

Figure 9. Summary of Phenotypes of *dich* and *cyc*

(A) In wild type, *dich* and *cyc* are needed together to control full dorsoventral asymmetry. The dorsal half (Dd) of each dorsal petal (dark blue) expresses both *cyc* and *dich*, while the lateral half (Dl) expresses only *cyc* (light blue).

(B) In the *dich* mutant, asymmetry in the dorsal petals is reduced.

(C) In the *backpetals* mutant (*cyc-705*), *cyc* is ectopically expressed so that petals in the lateral and ventral positions resemble mirror-image duplication of the lateral half of the dorsal petal (light blue). However, the asymmetry of the dorsal petal is unchanged, since the activity of *dich* is unaffected.

initial asymmetry, which may have had a particular role in early meristem development, could then have been recruited and built upon several times independently during evolution to generate organ asymmetry later in development.

Experimental Procedures

Plant Materials

Plant growth conditions were as previously described (Carpenter et al., 1987). Stocks JI 98 and Sippe 50 were used as standard wild types for comparisons with mutants. The origin of *dich*^{G} (obtained from Gatersleben, Germany), *dich-25*, *dich-717*, and *dich-718* have been described previously (Luo et al., 1996). The *backpetals* mutant was a spontaneous mutation, obtained from the JI98 genetic background. To reveal venation patterns, flowering spikes were cut off and the stems placed in blue or green ink for several hours. Lobes were then dissected from flowers and flattened between two glass slides before scanning into a computer and enhancing the regions colored with ink. SEMs were made on plastic replicas as described previously (Carpenter et al., 1995).

DNA Analysis

DNA extraction and blots were conducted as described previously (Luo et al., 1991). An EcoRI fragment containing the ORF of *cyc* (prepared from pJAM2118) was used as a probe to screen a cDNA library, made from young inflorescences of wild-type plants (Simon et al., 1994). Hybridization and washing were at moderate stringency (60°C, 1× SSC, 0.5% SDS). From about 2×10^6 recombinants, a cDNA clone (pJAM2078) was obtained, which contained the ORF of *dich*. The full length of the *dich* transcribed region was determined by 3′ and 5′ RACE PCR (5′ RACE system: GIBCO–BRL). The ORF in pJAM2078 was used to screen a genomic library of wild-type *Antirrhinum* DNA, and two overlapping clones, pJAM2236 and pJAM2237, with insert sizes of 13 kb and 14 kb respectively, were isolated. Two EcoRI fragment in the 14 kb insert of pJAM2237 were subcloned into Bluescript KS$^+$ to give pJAM2130 and pJAM2131, and sequenced by the dideoxynucleotide method. When the sequence was compared to that of the *dich* cDNA, two exons were identified and one of them contained the uninterrupted ORF of *dich*.

Restriction enzyme mapping (EcoRI, EcoRV, HindIII, PstI, SstI, and XhoI) was conducted to detect the alterations in *dich* among

different *dich* mutants. The precise insertion site of the transposon in *dich*^{G} was determined by inverse PCR. DNA from *dich*^{G} plants was digested with XhoI and then self-ligated; the circularized XhoI fragments were used as templates in a PCR amplification with a pair of outward-pointing primers, G4262 (5′-GTTCGTCCCACCAAC GTCGTG-3′) and G2198 (5′-GCGGACTTGCCTTATATTGG-3′), which were designed according to the *dich* sequence adjacent to the transposon; subsequently, a fragment containing the left end of the transposon (with respect to the *dich* gene) and its adjacent *dich* sequence was amplified and cloned to give a plasmid, pJAM2115. This plasmid was partially sequenced, and the internal sequence of the transposon was used to design primer G4312 (5′-GCACGAACAA TTCTTTCTCGAG-3′), so as to obtain the sequence of the right end of the transposon. With primers G4312 and G2192 (a *dich*-specific primer, 5′-CTAATTGATGAACTTATGCTGAT-3′), PCR was conducted to amplify the other end of the transposon and its adjacent *dich* sequence. The PCR product was cloned to give plasmid pJAM2117, which was partially sequenced to confirm the insertion site of the transposon.

To analyze the *backpetals* mutant, a 1.5 kb EcoRI fragment specific to the mutant was cloned into lambda gt10 vector (Amersham PRN1713, N334L) to give clone pJAM2238, which contained the right end of the transposon adjacent to sequence from the *cyc* locus. Inverse PCR was used to clone the other end of the transposon and its adjacent sequence as follows. DNA from the *backpetals* plants was digested with EcoRI and self-ligated; the circularized EcoRI fragments were used as templates in a PCR amplification, using a pair of primers, G3990 (5′-CTCAATCTCCCTACATATAC-3′) and G3988 (5′-CTGCCCCACTGCTTAGTGAAC-3′), which were designed according to the *cyc* sequence presumed to be adjacent to the left end of the transposon. A fragment containing the left end of the transposon and its adjacent sequence was amplified, cloned to give plasmid pJAM2240, and sequenced.

The sequence of the *cyc* locus around the transposon insertion site in *backpetals* mutant and its progenitor was further analyzed by PCR and restriction mapping. Both the *backpetals* mutant and its wild-type progenitor carried a 1.2 kb transposon insertion about 4.5 kb upstream of the *cyc* transcribed region. This insertion was not found in another wild-type line (JI75) and may simply represent a polymorphism present in some wild-type stocks. To analyze the derivative of the *backpetals* mutant carrying an imprecise excision, PCR was used to amplify the DNA footprint with a pair of primers on either side, G3988 (5′-CTGCCCCACTGCTTAGTGAAC-3′) and G3883 (5′-CGATTGTACTACTTTAAAGGGAC-3′). The resulting 0.57 kb fragment was cloned to give plasmid pJAM2241 and sequenced.

RNA Analysis

To prepare total RNA from lobes, flower buds at various developmental stages were collected. Lobes of the ventral petal and one lateral petal from ten flower buds of the same length were dissected and pooled separately. The dorsal lobes from ten flower buds were further dissected into dorsal (Dd) and lateral (Dl) halves (see Figure 6) before being pooled separately. First-strand cDNA was synthesized using AMV transcriptase (Boehringer Mannheim) with primer B26 (5′-GACTCGAGTCGACATCGA$(T)_{17}$-3′). 3′ RACE PCR was then carried out to detect *cyc* and *dich* transcripts, with primer B25 (5′-GACTCGAGTCGACATCG-3′) and a degenerate primer G873 based on a conserved region of the TCP domain (5′-ATGCTIGGITT (T/C)GA(T/C)AA(A/G)CCIAG(T/C)AA(A/G)ACICTIGA(T/C)TGG-3′). The transcript of *def* (Sommer et al., 1990) was detected as a control, with primer B25 and a *def*-specific primer G344 (5′-CTTATCACAGTTTTA GGAAAG-3′). PCR was carried out as described previously (Ingram et al., 1997), with annealing temperature of 55°C, and 35 cycles. The PCR products were separated by electrophoresis, blotted, and probed with the ORFs of *dich*, *cyc*, or *def* at high stringency.

The methods for digoxigenin labeling of RNA probes, tissue preparation, and in situ hybridization were as described previously (Coen et al., 1990). The probe used to detect the *cyc* transcript was prepared as previously described (Luo et al., 1996). A plasmid, pJAM2143, containing a 0.45 kb fragment from the 5′ end of *dich* cDNA, was used to generate templates for preparation of either antisense or sense probes.

Acknowledgments

We would like to thank Gatsby Charitable Foundation for its support. We also thank Desmond Bradley, Jorge Almeida, and Emma Keck for helpful comments on the manuscript.

Received August 25, 1999; revised October 24, 1999.

References

Almeida, J., Rocheta, M., and Galego, L. (1997). Genetic control of flower shape in *Antirrhinum majus*. Development *124*, 1387–1392.

Busturia, A., and Bienz, M. (1993). Silencers in *Abdominal-B*, a homeotic *Drosophila* gene. EMBO J. *12*, 1415–1425.

Carpenter, R., and Coen, E.S. (1990). Floral homeotic mutations produced by transposon-mutagenesis in *Antirrhinum majus*. Genes Dev. *4*, 1483–1493.

Carpenter, R., Martin, C., and Coen, E.S. (1987). Comparison of genetic behaviour of the transposable element Tam3 at two unlinked pigment loci in *Antirrhinum majus*. MGG *207*, 82–89.

Carpenter, R., Copsey, L., Vincent, C., Doyle, S., Magrath, R., and Coen, E. (1995). Control of flower development and phyllotaxy by meristem identity genes in *Antirrhinum*. Plant Cell *7*, 2001–2011.

Celniker, S.E., Sharma, S., Keelan, D.J., and Lewis, E.B. (1990). The molecular genetics of the bithorax complex of *Drosophila*: *cis*-regulation in the *Abdominal-B* domain. EMBO J. *9*, 4277–4286.

Charlton, W.A. (1998). Pendulum symmetry. In Symmetry in Plants, R.B. Jean and D. Barabe, eds. (Singapore: World Scientific Publishing Co.), pp. 61–87.

Coen, E.S. (1996). Floral symmetry. EMBO J. *15*, 6777–6788.

Coen, E.S., Romero, J.M., Doyle, S., Elliott, R., Murphy, G., and Carpenter, R. (1990). *floricaula*: a homeotic gene required for flower development in *Antirrhinum majus*. Cell *63*, 1311–1322.

Cubas, P., Lauter, N., Doebley, J., and Coen, E. (1999). The TCP domain: motif found in proteins regulating plant growth and development. Plant J. *18*, 215–222.

Dingwall, C., and Laskey, R.A. (1991). Nuclear targeting sequences: a consensus? TIBS *16*, 478–481.

Doebley, J., Stec, A., and Hubbard, L. (1997). The evolution of apical dominance in maize. Nature *386*, 485–488.

Goodrich, J., Puangsomlee, P., Martin, M., Long, D., Meyerowitz, E.M., and Coupland, G. (1997). A Polycomb-group gene regulates homeotic gene expression in *Arabidopsis*. Nature *386*, 44–51.

Gyurkovics, H., Gausz, J., Kummer, J., and Karch, F. (1990). A new homeotic mutation in the *Drosophila* bithorax complex removes a boundary separating two domains of regulation. EMBO J. *9*, 2579–2585.

Ingram, G.C., Doyle, S., Carpenter, R., Schultz, E.A., Simon, R., and Coen, E.S. (1997). Dual role for *fimbriata* in regulating floral homeotic genes and cell division in *Antirrhinum*. EMBO J. *21*, 6521–6534.

Kosugi, S., and Ohashi, Y. (1997). PCF1 and PCF2 specifically bind to *cis* elements in the rice proliferating cell nuclear antigen gene. Plant Cell *9*, 1607–1619.

Kuckuck, H., and Schick, R. (1930). Die erbfaktoren bei *Antirrhinum majus* und ihre bezeichnung. Z. f. indukt. Abst. -u. Vererbungsl. *56*, 51–83.

Luo, D., Coen, E.S., Doyle, S., and Carpenter, R. (1991). Pigmentation mutants produced by transposon mutagenesis in *Antirrhinum majus*. Plant J. *1*, 59–69.

Luo, D., Carpenter, R., Vincent, C., Copsey, L., and Coen, E. (1996). Origin of floral asymmetry in *Antirrhinum*. Nature *383*, 794–799.

Mihaly, J., Hogga, I., Gausz, J., Gyurkovics, H., and Karch, F. (1997). In situ dissection of the *Fab-7* region of the bithorax complex into a chromatin domain boundary and a *Polycomb*-response element. Development *124*, 1809–1820.

Sanchez-Herrero, E. (1991). Control of the expression of the bithorax complex genes *Abdominal-A* and *Abdominal-B* by *cis*-regulatory regions in *Drosophila* embryos. Development *111*, 437–449.

Simon, J., Chiang, A., and Bender, W. (1992). Ten different *Polycomb*

group genes are required for spatial control of the *abdA* and *AbdB* homeotic products. Development *114*, 493–505.

Simon, R., Carpenter, R., Doyle, S., and Coen, E. (1994). *Fimbriata* controls flower development by mediating between meristem and organ indentity genes. Cell *78*, 99–107.

Sommer, H., Beltran, J-P., Huijser, P., Pape, H., Lonnig, W.-E., Saedler, H., and Schwarz-Sommer, Z. (1990). *Deficiens*, a homeotic gene involved in the control of flower morphogenesis in *Antirrhinum majus*: the protein shows homology to transcription factors. EMBO J. *9*, 605–613.

Stubbe, H. (1966). Genetik und Zytologie von Antirrhinum L. sect. Antirrhinum Veb (Jena: Gustav Fischer).

Wolpert, L., Beddington, R., Brockes, J., Jessell, T., Lawrence, P., and Meyerowitz, E. (1998). Principles of Development (Oxford: Current Biology Ltd. and Oxford University Press).

Zink, D., and Paro, R. (1995). *Drosophila* Polycomb-group regulated chromatin inhibits the accessibility of a *trans*-activator to its target DNA. EMBO J. *14*, 5660–5671.

GenBank Accession Number

The accession number for *dichotoma* is AF199465.